PHYSICAL REVIEW B VOLUME 30, NUMBER 10 15 NOVEMBER 1984

Interpretation of deep-level optical spectroscopy and deep-level transient spectroscopy data: Application to irradiation defects in GaAs

S. Loualiche

Centre National d'Etude des Télécommunications, Route de Tregastel, 22301 Lannion Cedex, France

A. Nouailhat and G. Guillot

Laboratoire de Physique de la Matière, Institut National des Sciences Appliquées de Lyon, 20 avenue Albert Einstein, 69621 Villeurbanne Cedex, France

M. Lannoo

Laboratoire de Physique des Solides, Institut Supérieur d'Electronique du Nord, 3 rue François Baës, 59046 Lille Cedex, France*

(Received 27 February 1984)

A detailed theoretical analysis of deep-level transient spectroscopy and deep-level optical spectroscopy data is worked out with application to some irradiation centers in GaAs. A simple model including the local point-defect symmetry is proposed to deduce from experiment the physical parameters characterizing the defects. The originality of the proposed method is to extract from the experimental results quantities corresponding to "ionization energies at zero distortion," which are directly comparable to the predictions of available theoretical calculations. For this the optical line-shape function is represented by a Gaussian curve adjusted to reproduce the exact first two moments, in the case of degenerate electronic states. An application is made to the case of E_1 and E_2 in GaAs where the hypothesis that these centers correspond to two consecutive charge states of the arsenic vacancy $V_{\rm As}$ is explored. Comparison between theory and experiment strongly supports the identification of E_1 and E_2 with $V_{\rm As}^{2-}$ and $V_{\rm As}^{-}$, respectively.

I. INTRODUCTION

The deep-level optical spectroscopy (DLOS) technique represents a major improvement in the measurement of optical ionization cross sections of defects in semiconductors. It is an extension of the deep-level transient spectroscopy (DLTS) technique of Lang[1] to include optical excitation, and it has more sensitivity and selectivity than conventional optical methods, such as optical absorption, photocapacitance, photoluminescence, etc. It was used by Henry and Lang[2] to measure the ionization cross section for GaP:O and was clarified and compared to other optical techniques by Chantre *et al.*,[3] who labeled it DLOS. In spite of these advantages and the fact that it provides a bridge between optical and electrical methods,[4] the main weakness of DLOS is that it is more dependent than other methods on the theoretical model used to extract the physical information.

There have already been several attempts to calculate the optical ionization cross sections using simplified theoretical models[3,5-9] which could help in the modelization of experimental results. The difficulty here is to find the best compromise between simplicity and accuracy of the model in order for the defect parameters which are extracted to have physical sense. Some of the difficulties lie (i) in the description of the wave function for the initial and final states of the defect, and (ii) in the way one incorporates the effect of the electron-lattice interaction which is known to play a fundamental role for many point defects. All approximate expressions which have been used factorize the optical cross section into a purely electronic part and a vibrational broadening function resulting from the electron-lattice interaction. They also assume that coupling to phonons occurs only with one local lattice mode, which allows one to describe the situation in terms of a simple configuration-coordinate diagram. Finally, this lattice mode is taken to have the same frequency in the initial and final states, an approximation which obviously is not correct in general, as illustrated experimentally by the system GaP:O.[2]

In this context the originality of the present work is to propose a theoretical model allowing one to extract, from experimental data, physical parameters which are directly comparable to the predictions of first-principles calculations.[10] This is the case, for instance, of the extension of the deep-level wave function, but our central result here will concern the "ionization energy at zero distortion." Such information can be obtained from the knowledge of the thermal-ionization energies (DLTS) and from a fit to the experimental curve of the photoionization cross section versus frequency (DLOS). A detailed application of the procedure is worked out for the irradiation centers E_1 and E_2 in GaAs. In this case we test the hypothesis that E_1 and E_2 correspond to two consecutive charge states of the arsenic vacancy $V_{\rm As}$, and we find that their respective identification to $V_{\rm As}^{2-}$ and $V_{\rm As}^{-}$ is strongly supported by the comparison between theory and experiment.

In Sec. II we describe how the general expression for σ is simplified by factorization and modelization of the electronic and vibrational parts, taking into account the sym-

 ©1984 The American Physical Society

metry properties of the defect. An example of fit to experimental data is presented for an irradiation center in GaAs to illustrate the interest of the technique. In Sec. III we show how the "ionization energies at zero distortion" can be obtained and apply the method to the case of E_1 and E_2. We present experimental evidence that E_1 and E_2 correspond to intrinsic defects and examine in detail their interpretation in terms of lattice vacancies.

II. THEORETICAL MODELS FOR THE OPTICAL CROSS SECTION

We first present the general basis of the treatment where the optical cross section is the convolution of an electronic part by an optical line-shape function and discuss the techniques used to modelize these two parts. We give details for two types of allowed transitions with different symmetries. Finally, we discuss the validity of the fitting procedure.

A. General basis of the models

The calculation of the photoionization cross section $\sigma(E)$ is based on the Fermi golden rule,

$$\sigma(E) \propto \frac{1}{E} \underset{i}{\mathrm{Av}} \left[\sum_f |\langle \phi_f | \vec{A}\cdot\vec{p} | \phi_i \rangle|^2 \delta(E-(E_f-E_i)) \right], \quad (1)$$

where Av_i denotes a thermal average over the initial states, and E is the energy $h\nu$ at which the optical transition between the initial state ϕ_i and the final state ϕ_f occurs. In this expression, $\vec{A}$ is the vector potential and $\vec{p}$ is the impulsion of the electron. In general, ϕ_i and ϕ_f are vibronic states. Using the adiabatic approximation and following the method due to Huang and Rhys,[11] we can write $\sigma(E)$ under the simplified form

$$\sigma(E) \propto \frac{1}{E} \sum_{n,\vec{k}} |\langle \psi_{n,\vec{k}} | \vec{A}\cdot\vec{p} | \psi_d \rangle|^2 S_{n,\vec{k}}(E) . \quad (2)$$

Here, ψ_d is the defect electronic wave function and $\psi_{n,\vec{k}}$ is the Bloch wave function of wave vector $\vec{k}$ belonging to band n, of energy $E_n(\vec{k})$. This already is an approximation since, in the general case, the band wave functions are modified by the presence of the defect, the effect being nonnegligible.[12] However, it is difficult to improve this approximation if one wishes to obtain a simple model from which a fit to experiment is possible, and thus no realistic calculation has been done up to now incorporating this effect. For the vibrational broadening function $S_{n,\vec{k}}(E)$ we take a Gaussian form,

$$S_{n,\vec{k}}(E) = (2\pi m_2)^{-1/2} \exp\left[-\frac{[E-E_n(\vec{k})-m_1]^2}{2m_2} \right], \quad (3)$$

with the origin for $E_n(\vec{k})$ taken at the absolute extremum of either the conduction or the valence band. Such a simplified expression only holds under certain conditions (i.e., strong-coupling or high-temperature limit) which are often realized for deep-level centers, so that it has been largely used in the literature.[1,3,13,14] We shall discuss its validity in more detail in Sec. III considering the specific example of E_1 and E_2. The two quantities m_1 and m_2 are the first and second moments of the optical line-shape function which turn out to have the following simple expressions (see, for instance, Ref. 2),

$$m_1 = E_T + d_{\mathrm{FC}} \quad (4)$$

and

$$m_2 = \hbar\omega\, d_{\mathrm{FC}}(2\bar{n}+1) , \quad (5)$$

in the case of transitions between two nondegenerate electronic states and assuming an average phonon frequency ω. In this expression, E_T is the threshold energy for zero-phonon transitions, d_{FC} is the Franck-Condon shift (see Fig. 1), and $\bar{n}$ is the Boltzmann factor,

$$\bar{n} = \left[\exp\frac{\hbar\omega}{k_B T} - 1 \right]^{-1} . \quad (6)$$

At high temperatures (condition realized for $T > 100$ K in GaAs), expression (3) of $S_{n,\vec{k}}(E)$ can be simplified further to give

$$S_{n,\vec{k}}(E) = (4\pi k_B T d_{\mathrm{FC}})^{-1/2} \times \exp\left[-\frac{[E-E_n(\vec{k})-E_T-d_{\mathrm{FC}}]^2}{4k_B T d_{\mathrm{FC}}} \right] . \quad (7)$$

It is this expression which we shall use in the following in order to fit the experimental curve $\sigma(E)$.

Long ago,[5] simplified models for the photoionization cross sections were derived to describe the experimental situation in terms of a restricted number of physically meaningful parameters. Lucovsky's model[6] has been largely used and is still in current use,[15] but it completely neglects the electron-lattice interaction. Chantre[16] has classified the existing models as taking into account this interaction[3,13,14,17,18] or neglecting it.[5,6,7,19,20] Those of the last group cannot describe the experimentally observed

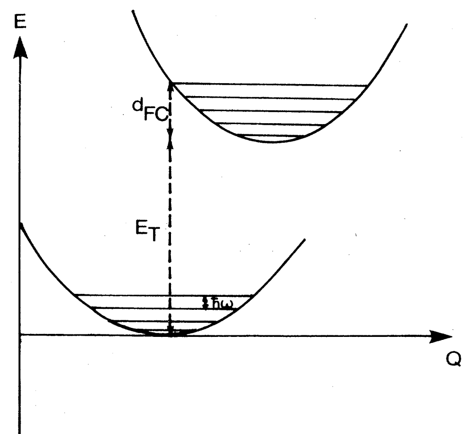

FIG. 1. Single configuration-coordinate diagram for nondegenerate electronic states interacting with one lattice mode.

broadening of $\sigma(E)$,[21] while the others are usually too simplified to reproduce $\sigma(E)$ over all of its spectral extension.[3]

From the theoretical point of view, the model due to Chantre[3,16] is a combination of Jaros's model[13] for the inclusion of the electron-lattice coupling and of the one derived by Monemar and Samuelson[14] to calculate the electronic matrix element. Its success is that it describes the photoionization curves over the entire energy range. Indeed, Chantre was able to show that the electronic transition did occur not only from the defect level to the minimum $\Gamma(\vec{k}=\vec{0})$ of the conduction band, but also to the other minima at point L $[\vec{k}=(2\pi/a)(1,1,1)]$ and at point X $[\vec{k}=(2\pi/a)(0,0,1)]$ (Fig. 2), an important feature which had been neglected before. This approach has greatly clarified the understanding of the photocapacitance results for which such transitions were believed to originate from different defects. DLOS experiments have shown that these results correspond, in fact, to transitions between the same defect level and different conduction-band minima.

To obtain an improved model, our theoretical expression for $\sigma(E)$ will be given by Eqs. (2) and (7), where we shall take into account the symmetry properties of the states in the calculation of the electronic matrix element. As in previous treatments we take here a simple form for the defect wave function ψ_d, but with well-defined symmetry properties (pure s, p, or d wave function). We then consider the transition toward one given extremum of band n at $\vec{k}=\vec{k}_n$, for which we write the wave function in the form

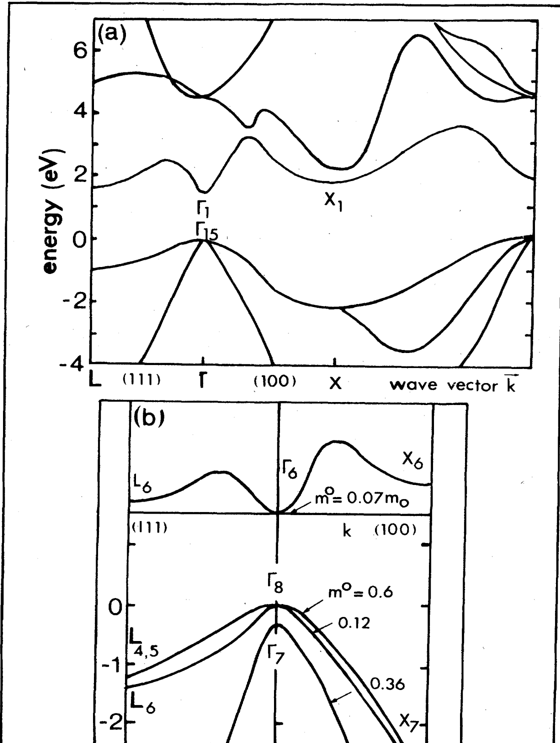

FIG. 2. Band structure of GaAs: (a) without spin-orbit coupling; (b) taking spin-orbit coupling into account.

$$\psi_{n,\vec{k}}=e^{i(\vec{k}-\vec{k}_n)\cdot\vec{r}}f_n(\vec{r})\ , \tag{8}$$

where $f_n(\vec{r})$ will be taken as the simplest function of $\vec{r}$ having the correct symmetry properties at $\vec{k}=\vec{k}_n$. To illustrate our technique we now consider some typical situations.

B. Transition from an "s"-like level to a "p"-like band

For the defect the simplest wave function is given by

$$\psi_d \propto e^{-\alpha r}\ . \tag{9}$$

The only allowed transition will occur towards the valence band whose maximum is at $\vec{k}_n=\vec{0}$. To simplify, we consider the strongly localized situation (where ψ_d only extends appreciably over the defect cell) and use a tight-binding approximation for $\psi_{n,\vec{k}}$, replacing $f_n(\vec{r})$ by $x_i\exp(-\lambda r)$, with $x_i=x$, y, or z (such an approximation will be justified later). This gives, for the Bloch functions,

$$\psi_i(\vec{k}) \propto x_i e^{-\lambda r} e^{i\vec{k}\cdot\vec{r}}\ . \tag{10}$$

From the two wave functions (9) and (10), it is easy to calculate all quantities $|\langle\psi_d|p_i|\psi_j(\vec{k})\rangle|^2$, where p_i is the ith component of $\vec{p}$. We must take the average of this quantity over all orientations, which gives

$$[\,|\langle\psi_d|p_i|\psi_j(\vec{k})\rangle|^2]_{\text{av}} \propto \frac{\alpha^2}{(s^2+k^2)^6}[(3s^2-k^2)^2+32k^4]\ , \tag{11}$$

where the quantity s is defined by

$$s=\alpha+\lambda\ , \tag{12}$$

and k^2 is the square modulus of $\vec{k}$.

In the absence of spin-orbit coupling the top of the valence band in GaAs has sixfold degeneracy (including spin). As shown on Fig. 2, spin-orbit coupling splits the valence band. The states at $\vec{k}=\vec{0}$ are of symmetry Γ_8 and Γ_7, and have, respectively, fourfold and twofold degeneracies.[22] However, this does not change the result (11) of our model calculation, since each function contributes in an identical way.[23] There will thus be only an effect due to the density of states, the Γ_8 subband giving twice the contribution of Γ_7. This is an important test in practice, since, if the experimental value of σ attributed to Γ_8 is about twice the Γ_7 value, then this is an indication that one has a transition due to an s state.

Let us conclude this case by giving the entire expression of σ as obtained from (2) combined with (7). We obtain the simple analytic formula

$$\sigma=\sigma_{\Gamma_8}+0.5C^{5/2}\sigma_{\Gamma_7}\ , \tag{13}$$

each σ_i being given by

$$\sigma_i=\frac{A}{y}\int_0^\infty \frac{x^{1/2}}{(x+e_{s,i})^6}[(3e_{s,i}-x)^2+32x^2]e^{-(y-e_i-x)^2}dx\ , \tag{14}$$

i standing for Γ_7 or Γ_8, A being a normalization coefficient, and all other symbols being defined as follows:

$$C = m_{\Gamma_8}/m_{\Gamma_7},\ \ x = \hbar^2 k^2/2m_i u$$

in each subband, and

$$y = h\nu/u,\ \ e_{s,i} = \hbar^2 s^2/2m_i u,\ \ e_i = E_{\text{op}} + \Delta_i/u,$$
$$u = (4k_B T d_{\text{FC}})^{1/2}\ , \tag{15}$$
$$\Delta_{\Gamma_8} = 0\text{eV} \ \text{and}\ \Delta_{\Gamma_7} = 0.35 \text{ eV for GaAs}\ ,$$

E_{op} being the optical threshold. To obtain this expression for σ we have replaced the sum in (2) by an integral and introduced the corresponding densities of states.

This result for the photoionization cross section has been applied to a deep level created by irradiation with 1-MeV electrons in vapor-phase-epitaxy (VPE) p-type GaAs.[24] This center gives rise to a level E_T located about 0.71 eV above the top of the valence band. It can also be obtained in liquid-phase-epitaxy (LPE) samples, but with a strong irradiation dose ($>10^{16}\ e\ \text{cm}^{-2}$). It corresponds to the case discussed above, i.e., the contribution of the Γ_8 subband is twice as intense as the Γ_7 one. The fit to experiment has been obtained by using expressions (13) and (14) with only two adjustable parameters: the Franck-Condon shift d_{FC} and the combined extension s of the defect and Bloch-state wave functions. The quality obtained from such a fit is reasonable, as shown by Fig. 3. The corresponding parameters are

$$d_{\text{FC}} = 0.12 \text{ eV},\ \ s^{-1} = 3.5\ \text{Å}\ . \tag{16}$$

It is interesting to note that the values obtained for d_{FC} are insensitive to the details of the model used to simulate the electronic matrix element (for instance, a model based on a transition between a defect s state to an s-like—band extremum gives essentially the same value of d_{FC}). This is an important point which we discuss in Sec. II D.

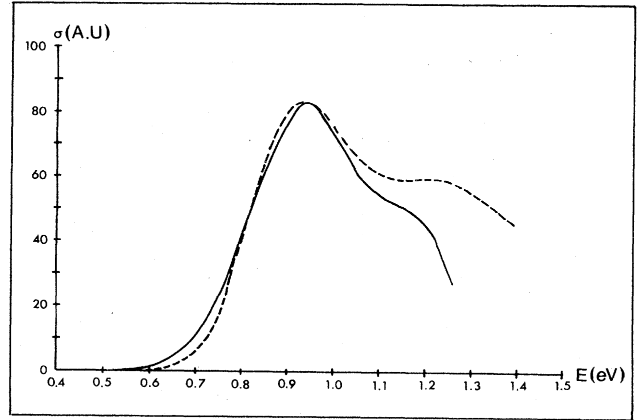

FIG. 3. Photoionization cross section versus energy for one irradiation center in p-type GaAs: solid line, experiment; dashed line, theory.

C. Transition from a "p" level to the conduction band

We proceed in a similar way as in Sec. II B, but take into account the characteristics of the conduction-band minima. In GaAs the eigenfunctions of the different minima at Γ, L, and X have well-defined symmetry properties.[25] Let us call A and B the atoms from which the III-V compound is built. The Γ_1 minimum corresponds to a combination of pure "s" functions s_A and s_B (in an s-p atomic-orbital picture). The L_1 minimum is a mixture of these "s" functions (s_A and s_B) and of (111) combinations of "p" functions [e.g., $(p_x+p_y+p_z)_{A,B}$]. As to the minimum X_1, its wave function is a combination of "s" states and "x"-like p states, for instance. To represent the defect state we use a trial p function of the simple form

$$\psi_{d,j} \propto x_j e^{-\alpha r}\ , \tag{17}$$

which we assume to be centered on a given lattice site. For the final states in the conduction band we again use Bloch functions as given by (8). We neglect the possible $\vec{k}$ dependence of $f_n(\vec{r})$ (this approximation will be discussed below) and, for our model, consider that only the "s" component of $f_n(\vec{r})$ on the defect site will contribute to the optical matrix element. This leads to the following expression for the "active" part $\psi_n^a(\vec{k})$ of the Bloch function:

$$\psi_n^a(\vec{k}) \propto e^{i(\vec{k}-\vec{k}_n)\cdot\vec{r}} e^{-\lambda r}\ . \tag{18}$$

The average square of the optical matrix element can be determined using the same technique as above, which leads to

$$[\,|\langle \psi_{d,j}\,|p_i\,|\,\psi_n^a(\vec{k})\rangle\,|^2]_{\text{av}} \propto \frac{s^2}{(s^2+k^2)^6}\{[3(s^2+k^2)-\epsilon(3s^2-k^2)]^2+32\epsilon^2k^4\}\ , \tag{19}$$

where now this expression depends on one extraparameter ϵ defined as $\epsilon=\alpha/s$. We now consider that the total photoionization cross section is the sum of contributions from regions around the points Γ, L, and X, which gives

$$\sigma = A(\sigma_\Gamma + P_L\sigma_L + P_X\sigma_X)\ , \tag{20}$$

where, in our simplified representation, P_L and P_X should represent the relative "s" character near points L and X (these two parameters are not calculated, but rather are deduced from the fit). Each individual σ_i is given by

$$\sigma_i = M_i C_i^{5/2}\frac{1}{y}\int_0^\infty \frac{x^{1/2}}{(x+e_{s,i})^6}\{[3(e_{s,i}+x)-\epsilon(3e_{s,i}-x)]^2+32\epsilon^2x^2\}\exp[-(y-e_i-x)^2]dx\ , \tag{21}$$

where M_i corresponds to the number of equivalent minima (three for point X and four for point L). Here the notation is the same as in (15), except that we have (see Table I for detailed values of the parameters in $Ga_{1-x}Al_xAs$)

$$C=m_\Gamma/m_i,\quad \Delta_\Gamma=0,\quad \Delta_L=0.29\text{ eV},\quad \Delta_X=0.46\text{ eV}\ . \tag{22}$$

Again, we obtain a simple analytical expression which we apply in Sec. III to the case of the E_1 and E_2 centers. Before this, we will discuss the validity of the models which we have introduced.

D. Reliability and justification of the models

The models which we have derived above essentially depend upon the following quantities.

(i) The functional form of the matrix element upon k^2, i.e., upon the energy in the corresponding subband.

(ii) The quantity m_1, which defines the average position of the Gaussian broadening function (7), representing the effect of the electron-lattice interaction.

(iii) The quantity k_BTd_{FC} itself, which defines the width of the Gaussian.

Let us first consider the approximations involved in the use of a Gaussian. This corresponds to the high-temperature regime of the strong-coupling case[26] and, in the simple case described above, m_1 and d_{FC} are related through Eq. (4). However, as discussed in Sec. III, it is always possible to approximate the broadening curve by a Gaussian having the correct first two moments of the spectral function. An important point concerns the sensitivity of the parameters m_1 and d_{FC} to the expression used for the electronic optical matrix element. The width in energy of the Gaussian is given by the quantity $u=(4k_BTd_{FC})^{1/2}$. From the experimental data reproduced later for E_1 and E_2, values for this quantity range from 0.06 to 0.09 eV. This is substantially weaker than the energy interval over which the fit is performed. It is then clear that m_1 should be relatively insensitive to the details of the model used for the optical matrix element, as confirmed by comparison of different models. This is less true for the value of $(4k_BTd_{FC})^{1/2}$, which, regardless, is more difficult to analyze in the general case.

Let us now try to justify our models for the optical matrix element. Expression (8) for the Bloch function near the extremum $\vec{k}=\vec{k}_n$ of the nth band corresponds, in fact, to the starting point of $\vec{k}\cdot\vec{p}$ theory, where it is written as

TABLE I. Experimental parameters used in the model calculation of the photoionization cross sections in $Ga_{1-x}Al_xAs$.

	$x=0.00$	$x=0.14$	$x=0.25$	$x=0.47$
E_{Γ_1} (eV)	1.424	1.605	1.750	2.082
E_{L_1} (eV)	$E_{\Gamma_1}+0.29$	$E_{\Gamma_1}+0.202$	$E_{\Gamma_1}+0.13$	$E_{\Gamma_1}-0.06$
E_{X_1} (eV)	$E_{\Gamma_1}+0.46$	$E_{\Gamma_1}+0.27$	$E_{\Gamma_1}+0.15$	$E_{\Gamma_1}-0.13$
E_g	1.424	1.605	1.750	1.952 (indirect)
$m^*_{\Gamma_1}$, $C_{\Gamma 1}$	0.067, 1	0.079, 1	0.088, 1	0.106, 1
$m^*_{L_1}$, C_{L1}	0.22, 0.3045	0.227, 0.348	0.233, 0.378	0.244, 0.434
$m^*_{X_1}$, C_{X1}	0.41, 0.1634	0.406, 0.195	0.403, 0.218	0.396, 0.268
M_{Γ_1}	1	1	1	1
M_{L_1}	4	4	4	4
M_{X_1}	3	3	3	3
$\hbar^2a^2/2m^*_{\Gamma_1}$ ($a^{-1}=1$ Å) (unit, 1 eV)	56.94	48.29	43.35	35.99
$M_{\Gamma_1}C^{5/2}_{\Gamma_1}$	1	1	1	1
$M_{L_1}C^{5/2}_{L_1}$	0.1	0.286	0.35	0.496
$M_{X_1}C^{5/2}_{X_1}$	0.032	0.05	0.067	0.11
$mC_{\Gamma_1}=e_s$	56.94	48.29	43.35	35.99
$mC_{L_1}=e_{sL}$	17.34	16.81	16.37	15.64
$mC_{X_1}=e_{sX}$	9.305	9.40	9.47	9.63

$$\psi_n(\vec{k},\vec{r})=e^{i(\vec{k}-\vec{k}_n)\cdot\vec{r}}\sum_m a_m(\vec{k})\psi_m(\vec{k}_n,\vec{r}) . \quad (23)$$

This shows that the function $f_n(\vec{r})$ depends on $\vec{k}$. At $\vec{k}=\vec{k}_n, a_n(\vec{k}_n)$ is equal to unity, whereas all other $a_m(\vec{k})$ vanish. Our first approximation is to assume that the rate of change of the $a_m(\vec{k})$ with $\vec{k}$ is small compared to the one due to $\exp[i(\vec{k}-\vec{k}_n)\cdot\vec{r}]$ itself. This is actually confirmed by the actual numbers, as discussed in Appendix A.

A second approximation is to consider that the function $f_n(\vec{r})$ [which is now equal to $\psi_n(\vec{k}_n,\vec{r})$] can be reduced to a simple "s"-like $[\exp(-\lambda r)]$ or "p"-like $[x_i \exp(-\lambda_r)]$ function centered on the defect site. This can be easily justified in the extreme tight-binding limit. In that case, $\psi_d(\vec{r})$ reduces to an atomic function at the defect site. If $f_n(\vec{r})=\psi_n(\vec{k}_n\vec{r})$ is itself expanded in terms of atomic orbitals, then only those centered on the defect site will interact with $\psi_d(\vec{r})$, and these can be represented approximately in terms of the simple "s" or "p" states used above. It was in this spirit that we introduced our simple models for the optical matrix elements. However, the parameter λ describing the decay of atomic orbitals is, for free atoms (using Slater rules, for instance[27]), of the order of 1.5 a.u. Here, from the values given in (16), we see that $\lambda < s = 0.14$ a.u., corresponding to a much weaker decay. This will be confirmed by the other cases discussed in Sec. III, where we shall find $\lambda = 0.06$ a.u., thus again much weaker than typical values in atomic orbitals.

This means that any serious justification of our model cannot be based on this tight-binding limit. Furthermore, the small values ($\alpha^{-1}=8$ Å) found for the decay constant in $\psi_d(\vec{r})$ suggest that an effective-mass-like approximation for the defect wave function might be more appropriate. In that case, α should characterize the decay constant of the envelope function. We show in Appendix B that such a formulation can indeed be used and cast in the form of our simple models, thereby bringing a more fundamental justification for their use.

III. EXTRACTION OF PHYSICAL PARAMETERS: APPLICATION TO E_1 AND E_2 IN GaAs

In this section we show how DLTS and DLOS data can be combined to obtain physical parameters characterizing the defect, the most important of which is the "ionization energy at zero distortion," e_T. We directly illustrate the procedure in the case of E_1 and E_2 in GaAs, for which we first summarize the known experimental results. We then relate the experimental quantities m_1 and E_T to e_T, whose value can be deduced from the fit to experimental data. This "experimental value" is finally compared, for E_1 and E_2, to predicted values for the arsenic vacancy V_{As}.

A. Summary of known experimental results

A large number of experimental results on irradiation defects in GaAs:n exist. However, despite this favorable situation their microscopic nature has not yet been firmly identified. This probably results from the lack of information about their local symmetry, which is a decisive element in their identification.[28]

The irradiation of n-type GaAs with electrons produces five electron centers and two hole centers (Fig. 4). The centers created at 4 K in GaAs:n do not differ from those created at 300 K, and their introduction rate does not depend on temperature.[29] They are found to anneal at 500 K (Ref. 30) and their annealing follows first-order kinetics (Refs. 31–33). This can be interpreted by a mechanism involving either close-pair recombination or dissociation[34,35] (recombination seems to be favored since no other defect is found to appear after the annealing of E_2 and E_3). The annealing rate of E_2 depends on the doping concentration, which has been shown to be a pure charge-state effect.[36]

These traps are thought to originate from simple intrinsic defects for the following reasons.

(1) They do not depend on the nature and concentration of doping impurities.[23]

(2) Their introduction rate is close to the theoretical value, with a threshold of 10 eV characteristic of the displacement of one atom.[37]

(3) They originate from the arsenic sublattice.[38,39]

(4) The concentration of E_1, E_2, and E_3 does not depend on x in $Ga_{1-x}Al_xAs$ ($x=0$ to 0.47).

This experimental evidence shows that E_1 and E_2 are intrinsic defects belonging to the As sublattice and having identical introduction rates[32,39,40] and annealing kinetics. They also have a behavior in $C(V)$ measurements which can simply be explained by assuming that they are acceptor centers[23,41] [note that Hall-effect and $C(V)$ data could also be explained by assuming E_1 to be an acceptor, and E_2 to be a donor plus deeper acceptors with a concentration of the order of E_2 (Ref. 42)]. It thus seems reasonable to believe that E_1 and E_2 are two charge states of the same intrinsic defect involving the arsenic vacancy V_{As} [this could be the vacancy alone, but also could be a complex such as $V_{As} + As_i$ (Ref. 42)].

Here we shall investigate the possibility of the isolated vacancy V_{As}. However, our results could still be relevant in a more complex situation such as $V_{As} + As_i$, provided the interaction between the two defects is not too strong.

B. Photoionization cross sections for E_1 and E_2

For E_1 and E_2 we have been able to measure the ionization cross section σ_{n0} (between the defect level and the

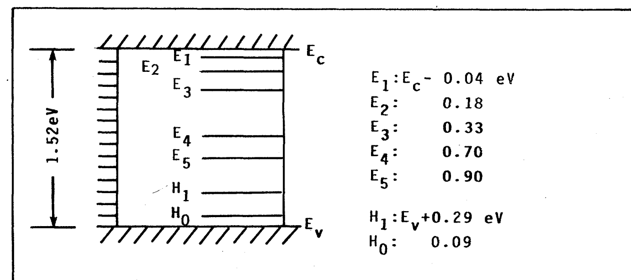

FIG. 4. Gap levels resulting from electron irradiation in n-type GaAs.

conduction band), but not σ_{p0} (between the defect level and the valence band). This might be due to the fact that this last transition is not allowed by symmetry. As the top of the valence band has local p character, this can be taken as an indication that the defect state has similar local symmetry. This is coherent with the identification of E_1 and E_2 with V_{As}, since it is known theoretically[43] that the vacancy level has T_2 symmetry (corresponding in the simplest case to local p character). We shall thus discuss the DLOS results for σ_{n0} by using the model leading to Eqs. (20) and (21) for a transition between a "p" level and the conduction bands.

As E_1 and E_2 correspond to the same center, we have assumed that they have equal values for the quantities P_L, P_X, α, and s in GaAs [in these compounds we have also assumed $\alpha(x)$ to be independent of x]. In this way the experimental results are well reproduced by the expression

$$\sigma = A(\sigma_{\Gamma 1} + 0.2\sigma_{L1} + 0.1\sigma_{X1}) . \tag{24}$$

The quality of the fit is illustrated on Fig. 5 for E_1 and on Fig. 6 for E_2. They correspond, respectively, to the model parameters of Tables II and III. In these tables the theoretical temperatures T_{th} are those producing the best fit for the term $u = (4k_B T d_{FC})^{1/2}$, where d_{FC} is the Franck-Condon shift defined above [as we shall see in Sec. III C, the fact that T_{th} is different from the experimental

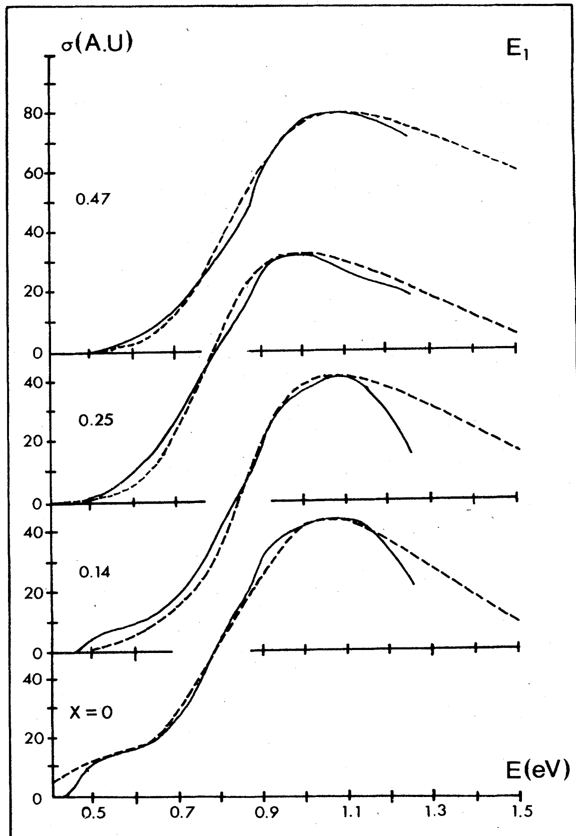

FIG. 5. Photoionization cross section versus energy corresponding to E_1 in $Ga_{1-x}Al_xAs$ for different values of x: solid line, experiment; dashed line, theory.

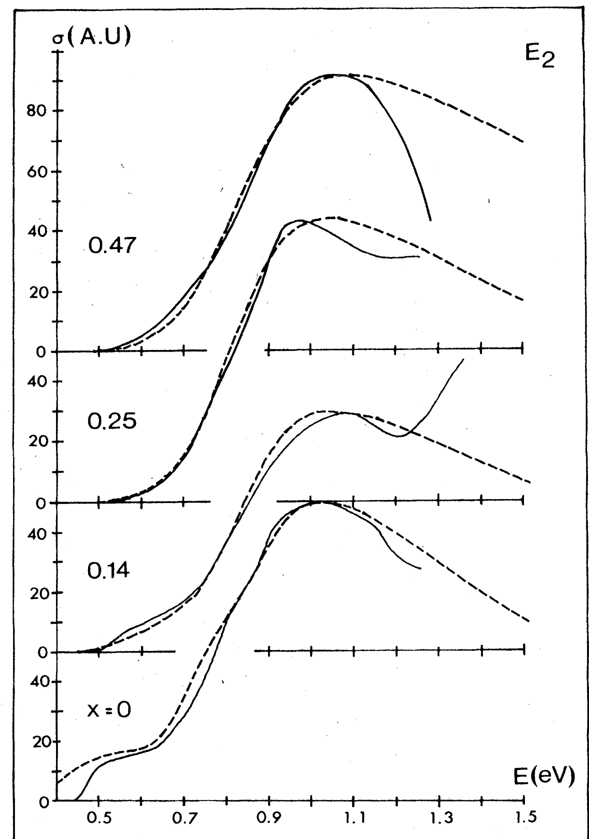

FIG. 6. Photoionization cross section versus energy corresponding to E_2 in $Ga_{1-x}Al_xAs$ for different values of x: solid line, experiment; dashed line, theory.

value is an indication that the simple model leading to expression (7) is not valid here]. It is interesting to analyze if the parameters of Tables III and IV do lead to reasonable physical situations. In a single configuration-coordinate diagram[26] the change Δq in the equilibrium value of the local lattice mode is related to the Franck-Condon shift d_{FC} by the simple relation

$$\tfrac{1}{2} M\omega^2 (\Delta q)^2 = d_{FC} , \tag{25}$$

In GaAs the mass of Ga and As is almost the same. To determine Δq we must then know the effective value of ω for this mode. Assuming the defect to be an arsenic vacancy V_{As}, we can use arguments derived in Ref. 44 to show that the effective frequency for a displacement involving nearest neighbors of the vacancy site is of the order of the transverse-acoustic frequency $\omega_{TA}(X)$ at point X, i.e., $\hbar\omega \simeq 10$ meV. Using this value and that of d_{FC} given in Tables II and III for GaAs, we easily obtain

$$\Delta q(E_1) \sim 0.6 \text{ Å}, \quad \Delta q(E_2) \sim 0.4 \text{ Å} , \tag{26}$$

Both values represent a reasonable order of magnitude for such displacements, confirming, to some extent, the coherence of our physical picture.

We now consider in more detail the microscopic models which could account for all the experimental information,

TABLE II. Model parameters deduced from the fit to experiment in the case of E_1.

	$x=0.00$	$x=0.14$	$x=0.25$	$x=0.47$
E_T (eV)	0.04	0.12	0.17	$0.30/X_1$ $0.43/\Gamma_1$
d_{FC} (eV)	0.38	0.48	0.45	0.45
s^{-1} (Å)	4	3.2	3.2	3.2
$\epsilon=\alpha/s$	0.5	0.4	0.4	0.4
α^{-1} (Å)	8	8	8	8
T_{expt} (K)	5	24	81	142
T_{th} (K)	60	60	81	142
$\hbar\omega$ (meV)	10	10		
A/σ_{max}	5.1×10^5	8.8×10^5	3.3×10^5	5.9×10^4
σ_{max} (10^{-18} cm^2)	6	30	170	7

i.e., the possibility that E_1 and E_2 are two charge states of the same defect, which we assume to be V_{As}. However, before doing this it is necessary to go beyond the simple model leading to expression (7). We show in the next section how the parameters of the Gaussian broadening functions can be calculated in the case of degenerate electronic states.

C. First moment of the optical line-shape function

The optical line-shape function $S_{n,\vec{k}}(E)$ occurring in Eq. (2) has been approximated in (3) and (7) by a Gaussian curve. This is exact only in the strong-coupling limit, or at high temperatures and for nondegenerate states.[26,45] Here we must consider more complex situations, where the electronic degeneracy of the system gives rise to Jahn-Teller distortions. In such cases a Gaussian curve can no longer represent the exact expression of the line-shape function. However, it can still represent a useful approximation to the exact function if one makes use of Eq. (3), where m_1 and m_2 are taken to be the first two moments of the exact curve. Such moments can be calculated directly, even when electronic degeneracy in the excited state is taken into account, as shown in Ref. 46.

TABLE III. Model parameters deduced from the fit to experiment in the case of E_2.

	$x=0.00$	$x=0.14$	$x=0.25$	$x=0.47$
E_T (eV)	0.18	0.20	0.34	$0.43/X_1$ $0.56/\Gamma_1$
d_{FC} (eV)	0.22	0.38	0.32	0.32
s^{-1} (Å)	4	3.2	3.2	3.2
$\epsilon=\alpha/s$	0.5	0.4	0.4	0.4
α^{-1} (Å)	8	8	8	8
T_{expt} (K)	32	78.5	116	192
T_{th} (K)	60	78.5	116	192
$\hbar\omega$ (meV)	10			
A/σ_{max}	1.8×10^6	6.9×10^5	3.7×10^5	7.5×10^4
σ_{max} (10^{-18} cm^2)	3	9	50	2

TABLE IV. Experimentally deduced ($e_T^{(e)}$) and theoretically predicted ($e_T^{(t)}$) values of the ionization energy at zero distortion.

	Model with		Model with	
	$V_{\rm As}^0$	$V_{\rm As}^-$	$V_{\rm As}^-$	$V_{\rm As}^{2-}$
Pair of charged states	(0, +)	(−, 0)	(−, 0)	(2−, −)
$e_T^{(e)}(i,f)$	−0.04	0.1	0.05	0.01
$e_T^{(t)}(i,f)$	0.52	0.27	0.27	0.02

Here we are, in principle, interested in defects for which there is electronic degeneracy and thus Jahn-Teller distortions both in the initial and final states. It is well known[26] that such systems exhibit several equivalent stable minima. We thus consider optical transitions from one such minimum of the initial state to all vibronic states derived from the electronically degenerate final state. The first two moments can then be calculated by the method described in Appendix C. However, the best parameter that can be deduced from the fit to experiment is m_1 and one can obtain its theoretical expression by using a very simple physical argument which we now produce. We then consider that both initial and final states are coupled to a set of lattice modes labeled by q_m and denote, by q_{mi}, the equilibrium value of each such lattice mode in the initial state. As usual, we consider that the quadratic terms $\frac{1}{2}k_m q_m^2$ are identical in both initial and final states, so that all energy differences depend only on the linear coupling coefficients. According to the Franck-Condon principle, the average transition occurs at $q_m = q_{mi}$ and the situation corresponds to the one depicted on Fig. 7. It can be seen on this figure that there are, in general, transitions to all components of the split final state. Here we make the simplifying assumption that, when averaging over equivalent minima and directions of polarization, each such transition contributes with an equal weight [preliminary calculations show that this is a good approximation for the cases we consider, i.e., $V_{\rm As}^-$ and $V_{\rm As}^{2-}$ (Ref. 47)]. Then the average transition will occur at the average energy of the degenerate excited state. For pure distortion modes the Jahn-Teller matrices are traceless matrices, so that, to first order, this average energy corresponds to the energy of the undistorted final state. Thus our conclusion is that m_1 is equal to the ionization energy at zero distortion, $e_T(i,f)$, plus the first-order energy gain in the initial state at one of its equilibrium configurations. As this last quantity is trivially equal to twice the Jahn-Teller energy $E_{\rm JT}^{(i)}$ in the initial state, we find the important result that

$$m_1 = e_T(i,f) + 2E_{\rm JT}^{(i)} \; . \tag{27}$$

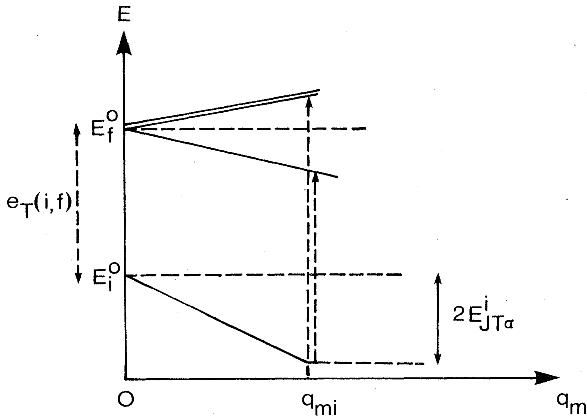

FIG. 7. Linear splitting or shift of the energy levels in the initial and final states versus the amplitude of the distortion mode q_m.

This reasoning is semiclassical and somewhat qualitative, but nevertheless it allows one to understand the physical origin of Eq. (27). We give, in Appendix C, a more general quantum-mechanical proof which also allows an extension to the determination of the higher-order moments m_n and, in particular, of m_2. It can be shown that there is no longer a simple relation between m_1 and m_2, as was the case in Eqs. (4) and (5). One might eventually question the use of a simple Gaussian curve for the situation depicted in Fig. 7 where the final state exhibits two separate branches (there, a superposition of two Gaussians, one for each branch, should be more appropriate). However, to be seen experimentally, the splitting between the two Gaussians must be larger than the sum of their individual half widths. This is not the case experimentally for E_1 and E_2, so that we have only considered one overall Gaussian curve. Its width is given by the second moment m_2, which is not equal to $2k_BT(m_1 - E_T)$, as would result from relations (4) and (5), which lead to (7). This is the reason why, in fitting with (7), we have been obliged to use a theoretical temperature $T_{\rm th}$ different from the experimental one. This is equivalent to the use of (3) with

$$m_1 = E_T + d_{\rm FC}, \quad m_2 = 2k_B T_{\rm th} d_{\rm FC} \; . \tag{28}$$

D. Discussion of the identification of E_1 and E_2 with $V_{\rm As}$

We shall base this discussion on a comparison between known experimental data and the possible theoretical arguments which one can obtain with confidence. From Secs. III A and III B it is obvious that a possible candidate to explain the properties of E_1 and E_2 is $V_{\rm As}$. As discussed before, the $C(V)$ measurements can be simply interpreted with the hypothesis that they are two consecutive acceptor states for which the most probable charge states would be $V_{\rm As}^-(E_2)$ and $V_{\rm As}^{2-}(E_1)$. We shall then first try to work out the consequences of such an assumption. It is well established[43] that the arsenic vacancy gives rise to two levels, one of A_1 symmetry found as a resonant state in the valence band, and the other of T_2 symmetry falling into the gap just below the bottom of the conduction band.

For the neutral vacancy $V_{\rm As}^0$ these levels must be populated with three electrons: two in A_1 and one in T_2. For $V_{\rm As}^-$ and $V_{\rm As}^{2-}$, one adds, respectively, one and two elec-

trons in T_2. From the similarity with $V_{\rm Si}$ one expects that substantial distortions will occur, either of tetragonal, trigonal, or mixed symmetry.[26] This favors the observation of a Franck-Condon shift, $d_{\rm FC}$. In addition, the symmetry of the state T_2 favors σ_{n0} over σ_{p0}, which is consistent with experiment.

Let us now discuss the experimental data concerning the electron-lattice interaction. For each center one knows (Tables II and III) E_T from DLTS data and m_1 from DLOS data. Theoretically, the latter quantity can be written in the form of Eq. (27), where $e_T(i,f)$ is the optical threshold for the undistorted vacancy and $E_{\rm JT}^{(i)}$ is the Jahn-Teller distortion energy in the initial state, i.e., before ionization (note that both quantities depend on the charge state). On the other hand, the DLTS energy E_T can be expressed as

$$E_T(i,f)=e_T(i,f)+E_{\rm JT}^{(i)}-E_{\rm JT}^{(f)} \ , \tag{29}$$

$E_{\rm JT}^{(f)}$ being the Jahn-Teller energy in the final state. From the experimental values of the quantity m_1-E_T, it is a very simple matter to show that

$$E_{\rm JT}^{(0)}+E_{\rm JT}^{(-)}=0.22 \text{ eV}, \quad E_{\rm JT}^{(-)}+E_{\rm JT}^{(2-)}=0.38 \text{ eV} \ , \tag{30}$$

where (0), $(-)$, and $(2-)$ designate the charge state. To proceed further, we must note that $V_{\rm As}$ should behave as $V_{\rm Si}$, but in different charge states ($V_{\rm As}^0=V_{\rm Si}^+$, $V_{\rm As}^-=V_{\rm Si}^0$, and $V_{\rm As}^{2-}=V_{\rm Si}^-$). If we accept this, $V_{\rm As}^0$ and $V_{\rm As}^-$ should distort tetragonally with $E_{\rm JT}^{(-)}\simeq 4E_{\rm JT}^{(0)}$.[26,48] From this relation, Eqs. (30) can be solved, leading to 0.045, 0.175, and 0.205 eV for $E_{\rm JT}^{(0)}$, $E_{\rm JT}^{(-)}$, and $E_{\rm JT}^{(2-)}$, respectively. Such values are quite reasonable, but smaller than in silicon. We can now insert these numbers into (27) or (29) and obtain an experimentally determined value for e_T in each case, i.e., $e_T^{(e)}(-,0)$ and $e_T^{(e)}(2-,-)$, where $(-,0)$ and $(2-,-)$ designate the pair of charge states involved in the ionization process. Both values are reported in Table IV, where they are compared to the results of pseudopotential local-density calculations[43] using Slater's transition-state argument. To evaluate these theoretical values $e_T^{(t)}$, we have taken for U, the Coulomb energy, a value 0.25 eV (identical to the silicon value), as obtained from a tight-binding determination.[49] The agreement between $e_T^{(e)}$ and $e_T^{(t)}$ is strikingly good, and we think that this represents a positive argument in favor of the identification of E_1 and E_2 with $V_{\rm As}^-$ and $V_{\rm As}^{2-}$.

It is tempting to apply the same considerations to another possible pair of charge states, e.g., $V_{\rm As}^0$ and $V_{\rm As}^-$ (in which E_1 would correspond to a single donor). The system of Eqs. (30) remains valid, but with (0), $(-)$, and $(2-)$ replaced by $(+)$, (0), and $(-)$. However, $V_{\rm As}^+$ has no electron in the T_2 state, and thus no Jahn-Teller energy. We thus obtain directly $E_{\rm JT}^{(0)}=0.22$ eV and $E_{\rm JT}^{(-)}=0.16$ eV (their ratio is no longer equal to 4, as in silicon). From these values we obtain $e_T^{(e)}(0,+)$ and $e_T^{(e)}(-,0)$, as given in Table IV, where they are again compared to the theoretical values. Clearly, the experimental values show no coherence since they are in inverted order (which cannot be explained) and now quite far from the expected values. Then the hypothesis of the two acceptor states $V_{\rm As}^-$ and $V_{\rm As}^{2-}$ seems more justified theoretically.

One consequence of the numerical values obtained for $V_{\rm As}^{2-}$ and $V_{\rm As}^-$ is that we predict, for the arsenic vacancy, a single donor level at about 0.5 eV from the conduction band. This level is not found experimentally. Preliminary calculations show that the corresponding capture cross section should be very small (in the 10^{-22}-cm^2 range), so that it has probably not been observed. One can also question whether or not the fact that E_2 is found to have a large capture cross section ($\sigma_n \simeq 10^{-13}$ cm^2) is in contradiction with its identification with a single acceptor. It will be shown in planned further work that this is compatible with the small ionization energy E_T found in this case. Finally, it is worth noticing that, with the values of the Jahn-Teller energies given above and a Coulomb energy U of 0.25 eV, the system formed by $V_{\rm As}^+$, $V_{\rm As}^0$, and $V_{\rm As}^-$ should not behave as a negative U center, contrary to what happens in silicon.[50]

IV. CONCLUSION

We have described in this work an original procedure allowing one to extract, from DLOS and DLTS data, physically important parameters which help in the determination of the microscopic nature of the defect. To do this we have shown how the modelization of the optical matrix elements can be improved by incorporating the symmetry properties of the defect, the effect of the electron-lattice interaction being incorporated through a Gaussian broadening function. Three important physical quantities can then be deduced from combined DLOS and DLTS experiments: the optical threshold energy, the DLTS energy level, and, to some extent, information on the localization of the defect wave function. From the two first pieces of information it is possible to derive an experimental value of the "ionization energy at zero distortion" which can be compared to theoretical predictions. The application of the method to E_1 and E_2 in GaAs leads to the conclusion that they can, respectively, be identified with $V_{\rm As}^{2-}$ and $V_{\rm As}^-$.

ACKNOWLEDGMENTS

The authors are grateful to M. Gavand and A. Laugier of the Laboratoire de Physique de la Matière, Institut National des Sciences Appliquées, for providing the liquid-phase-epitaxy samples. This work was supported by the Délégation Générale à la Recherche Scientifique et Technique (Contract No. 79-7-0724).

APPENDIX A

We must justify the neglect of terms such as $a_m(\vec{k})$ with $m\neq n$ in expression (23). For this we first use a simple two-band model for an extremum lying at $\vec{k}=\vec{0}$, which will allow one to derive simple useful orders of magnitude. Equation (23) can be written near $\vec{k}=\vec{0}$ as

$$\psi_v(\vec{k})=e^{i\vec{k}\cdot\vec{r}}[a_c(\vec{k})\psi_c(\vec{k}=\vec{0})+a_v(\vec{k})\psi_v(\vec{k}=\vec{0})] \ , \tag{A1}$$

where c and v denote the conduction and valence bands. Standard $\vec{k}\cdot\vec{p}$ theory applied to this case gives a 2×2 matrix,

$$\left[\frac{\hbar^2\vec{k}^2}{2m}+\frac{E_c+E_v}{2}\right]\mathbb{1}+\begin{bmatrix} E_g/2 & \frac{\hbar k}{m}M \\ \frac{\hbar k}{m}M^* & -E_g/2 \end{bmatrix}, \qquad (A2)$$

where M is the $\vec{k}\cdot\vec{p}$ matrix element and E_g is the energy gap. A second-order expansion of the energy gives the effective masses m_c and m_v,

$$m_c=\frac{m}{1+2|M|^2/mE_g}, \quad m_v=\frac{m}{-1+2|M|^2/mE_g}. \qquad (A3)$$

It is also possible to express $|a_c|^2$ and $|a_v|^2$ in terms of the parameters

$$|a_c|^2=\tfrac{1}{2}\left[1-\left[1+\frac{4\hbar^2|M|^2}{m^2E_g^2}k^2\right]^{-1/2}\right]$$

and (A4)

$$|a_v|^2=\tfrac{1}{2}\left[1+\left[1+\frac{4\hbar^2|M|^2}{m^2E_g^2}k^2\right]^{-1/2}\right].$$

The quantity of interest is the rate of change of $|a_c|^2$ and $|a_v|^2$ near $\vec{k}=\vec{0}$ (where $a_v=1$ and $a_c=0$). To obtain a change of 15% with respect to the values at $\vec{k}=\vec{0}$ in (A4) requires a value of $\vec{k}$ such that

$$\frac{4\hbar^2|M|^2}{m^2E_g^2}k^2=1. \qquad (A5)$$

Choosing for m_v the reasonable value $0.5m$ fixes $|M|$ in (A3) so that condition (A5) can also be written as

$$\frac{\hbar^2k^2}{2m_v}=\frac{E_g}{6}, \qquad (A6)$$

which is of the order of 0.25 eV for GaAs. Furthermore, the maximum variation of $|a_v|^2$ is limited to 0.5. This cannot explain the extremely fast change of the experimental $\sigma(E)$, where σ is reduced to half of its value for $\hbar^2k^2/2m_v$, equal to 0.06 eV for a defect with transitions to the valence band. Such conclusions have been confirmed more quantitatively in a recent calculation by Chaudhuri.[8]

APPENDIX B

We want to calculate the optical matrix element $I(\vec{k})$ between a defect state $\psi_d(\vec{r})$ and, for instance, a conduction-band wave function near the minimum $\vec{k}=\vec{k}_1$. For this we consider situations where ψ_d is sufficiently delocalized so that it can be expressed in the following form,

$$\psi_d(\vec{r})=F(\vec{r})\sum_n a_n\psi_{n;\vec{k}_n}(\vec{r}), \qquad (B1)$$

valid in the limit of effective-mass theory. Here, $F(\vec{r})$ is a variational envelope function, $\psi_{n;\vec{k}_n}$ being a Bloch state at the extremum of band n. Then $I(\vec{k})$ is given by

$$I(\vec{k})=\sum_n a_n\langle\psi_{c,\vec{k}}|p_i|F\psi_{n;\vec{k}_n}\rangle, \qquad (B2)$$

For $\vec{k}$ values such that $\vec{k}\sim\vec{k}_1$, and if one assumes that $F(\vec{r})$ is well delocalized in real space, then only terms such that $\vec{k}_n=\vec{k}_1$ will contribute, which gives

$$I(\vec{k})\simeq a_1\langle\psi_{c,\vec{k}}|p_i|F\psi_{c,\vec{k}_1}\rangle. \qquad (B3)$$

As discussed in the text and in Appendix A, we take

$$\psi_{c,\vec{k}}\simeq e^{i(\vec{k}-\vec{k}_1)\cdot\vec{r}}\psi_{c,\vec{k}_1}(\vec{r}), \qquad (B4)$$

which allows one to obtain $I(\vec{k})$ as the sum of two terms:

$$I(\vec{k})=a_1(\langle e^{i(\vec{k}-\vec{k}_1)\cdot\vec{r}}|\psi_{c,\vec{k}_1}|^2|p_i|F\rangle + \langle e^{i(\vec{k}-\vec{k}_1)\cdot\vec{r}}\psi_{c,\vec{k}_1}F|p_i|\psi_{c,\vec{k}_1}\rangle). \qquad (B5)$$

The second term is negligible. Indeed the Fourier expansion $\sum_{\vec{q}}F_{\vec{q}}e^{i\vec{q}\cdot\vec{r}}$ of F only involves small $\vec{q}$ vectors. This means that one must have $\vec{k}-\vec{k}_1=\vec{q}$, leaving the matrix element $\langle\psi_{c,\vec{k}_1}|p_i|\psi_{c,\vec{k}_1}\rangle$, which obviously vanishes. The first term of (B5) can be transformed by using the following argument: It is always possible to make the following expansion:

$$|\psi_{c,\vec{k}_1}|^2(p_iF)=b_0e^{-\lambda r}(p_iF)+\sum_{n\,(\neq 0)}b_nf_n(\vec{r}), \qquad (B6)$$

where the $f_n(\vec{r})$ are taken orthogonal to the first term on the right-hand side, $e^{-\lambda r}$ being chosen to have the maximum overlap between this term and the left-hand side. Then $e^{-\lambda r}(p_iF)$ represents the best approximation to the left-hand side of (B6), and one can write

$$I(\vec{k})\propto\langle e^{i(\vec{k}-\vec{k}_1)\cdot\vec{r}}e^{-\lambda r}|p_i|F\rangle. \qquad (B7)$$

In cases where F corresponds to a p function, this expression exactly corresponds to our approximate model of Eqs. (17) and (18), but at the condition of replacing ψ_d by the envelope function F. This has consequences concerning the physical meaning of decay constants. From (B7) it is apparent that λ has no particular significance, while the decay constant α in the approximate form $F\sim x_j\exp(-\alpha r)$ is a measure of the extension of the envelope function, i.e., also of the wave function ψ_d itself.

APPENDIX C

This appendix is devoted to a calculation of the moments of the line-shape function $S_{n,\vec{k}}(E)$ in the case of electronically degenerate states. The moment of order p of $E\sigma(E)$ can be written from Eq. (1) as

$$M_p=\underset{i}{\mathrm{Av}}\left[\sum_f|\langle\phi_f|\vec{A}\cdot\vec{p}|\phi_i\rangle|^2(E_f-E_i)^p\right]. \qquad (C1)$$

Here, ϕ_i and ϕ_f are vibronic wave functions which are, respectively, eigenfunctions of the Hamiltonian operators H_0 and H_1. The states $|\phi_f\rangle$ are derived from a degenerate electronic state of eigenstates $|\psi_e\rangle$. A complete basis set for $|\phi_f\rangle$ can thus be built from all products $|\psi_e\rangle|\chi_j\rangle$, where $|\chi_j\rangle$ is the jth vibrational eigenstate of the entire system in the undistorted situation. From

the closure relation, one obtains

$$\sum_f |\phi_f\rangle\langle\phi_f| = \sum_e |\psi_e\rangle\langle\psi_e| \quad \text{(C2)}$$

since the $|\chi_j\rangle$ form a complete set for the lattice problem. For $|\phi_i\rangle$ we consider the static limit where we can write

$$|\phi_i\rangle = |\psi_g\rangle\, |\chi_{g,l}\rangle ,$$

where $|\chi_{g,l}\rangle$ represents the vibrational eigenstates centered on a set of lattice positions which minimize the ground-state energy. We can thus write

$$M_p = \operatorname*{Av}_{g,l} \langle\chi_{g,l}| \sum_{e',e} \langle\psi_g|\vec{A}\cdot\vec{p}\,|\psi_{e'}\rangle\langle\psi_{e'}|(H_1-E_i)^p|\psi_e\rangle \times\langle\psi_e|\vec{A}\cdot\vec{p}\,|\psi_g\rangle|\chi_{g,l}\rangle . \quad \text{(C3)}$$

In this expression one has to average over the different minima in the ground state, and over the vibrational states, but also over the different polarization directions. This could be done in detail when one has a precise microscopic description of the defect. This is not the case here and all we can do is assume that the averaging procedure and the symmetry conditions are such that only terms with $e=e'$ survive, and that the average of $|\langle\psi_g|\vec{A}\cdot\vec{p}\,|\psi_e\rangle|^2$ is a constant independent of the pair of states g,e. This leads to

$$M_p = |\langle\psi_g|\vec{A}\cdot\vec{p}\,|\psi_e\rangle|^2 \operatorname*{Av}_{l}\left\langle\chi_{g,l}\left|\sum_e \langle\psi_e|(H_1-E_i)^p|\psi_e\rangle\right|\chi_{g,l}\right\rangle . \quad \text{(C4)}$$

It is only when the conditions leading to (C4) are met that $\sigma(E)$ (and all its moments) can be factorized into a purely electronic part and a vibrational one, $S_{n,\vec{k}}(E)$.

Our theoretical expression for the moments is thus completely coherent with the expression we have used to analyze the experimental results. With this we can calculate the reduced moments M_p/M_0,

$$M_p/M_0 = \operatorname*{Av}_{l} \langle\chi_{g,l}|\, t(H_1-E_i)^p\, |\chi_{g,l}\rangle , \quad \text{(C5)}$$

where t stands for a $1/g$ trace, where g is the degeneracy in the excited state. To evaluate the moments we have to know the expression of H_1 and H_0

$$H_1 = (E_f^0 + H_Q)I_f - \sum_\alpha V_\alpha q_\alpha, \quad H_0 = (E_i^0 + H_Q) - \sum_\alpha J_\alpha q_\alpha , \quad \text{(C6)}$$

where $E_{i,f}^0$ are the undistorted electronic energies, I_f is the unit matrix in the degenerate final electronic state, q_α is the distortion mode, V_α is electron-lattice interaction matrices of size $g\times g$, and J_α is the electron-lattice interaction parameters in the lower-energy branch of the initial state. With this, the calculation of $m_1 = M_1/M_0$ easily reduces to

$$m_1 = \operatorname*{Av}_{l} \langle\chi_{g,l}|(tH_1) - H_0|\chi_{g,l}\rangle , \quad \text{(C7)}$$

Using (C6) and the fact that, for pure distortion modes, the V_α are traceless matrices, one obtains

$$m_1 = E_f^0 - E_i^0 + \sum_\alpha J_\alpha q_{\alpha g} , \quad \text{(C8)}$$

where the $q_{\alpha g}$ correspond to the equilibrium values of the distortion modes. It is then a simple matter to show that, with $e_T(i,f) = E_f^0 - E_i^0$,

$$m_1 = e_T(i,f) + 2E_{\text{JT}}^{(i)} , \quad \text{(C9)}$$

which is the required expression. It is not trivial that the approximations leading to (C9) are always met in practice, but preliminary calculations show that they are well satisfied in our case.

*Laboratoire associé au Centre National de la Recherche Scientifique No. 253.

[1]D. V. Lang, J. Appl. Phys. **45**, 3023 (1974).
[2]C. H. Henry and D. V. Lang, Phys. Rev. B **15**, 989 (1977).
[3]A. Chantre, G. Vincent, and D. Bois, Phys. Rev. B **23**, 5335 (1981).
[4]P. Leyral, F. Litty, S. Loualiche, A. Nouailhat, and G. Guillot, Solid State Commun. **38**, 333 (1981).
[5]D. M. Eagles, J. Phys. Chem. Solids **16**, 76 (1960).
[6]G. Lucovsky, Solid State Commun. **3**, 299 (1965).
[7]H. B. Bebb, Phys. Rev. **185**, 1116 (1969).
[8]S. Chaudhuri, Phys. Rev. B **26**, 6593 (1982).
[9]S. Loualiche, A. Nouailhat, and G. Guillot, Physica **116B**, 474 (1983).
[10]A brief report of this work has been presented elsewhere: S. Loualiche, A. Nouailhat, and M. Lannoo, Solid State Commun. **51**, 509 (1984).
[11]K. Huang and A. Rhys, Proc. R. Soc. London, Ser. A **204**, 406 (1950).
[12]M. G. Burt, J. Phys. C **13**, 1825 (1980).
[13]M. Jaros, Phys. Rev. B **16**, 3694 (1977).
[14]B. Monemar and L. Samuelson, Phys. Rev. B **18**, 809 (1977).
[15]L. A. Ledebo (private communication).
[16]A. Chantre, Ph.D. thesis, Grenoble University, 1979.
[17]A. A. Kopylov and A. N. Pikhtin, Fiz. Tverd. Tela (Leningrad) **16**, 1837 (1974) [Sov. Phys. Solid State **16**, 1200 (1975)].
[18]B. K. Ridley, J. Phys. C **13**, 2015 (1980).
[19]S. T. Pantelides and J. Bernholc, in *Proceedings of the International Conference on Radiation Effects in Semiconductors, Dubrovnik, 1976*, edited by N. B. Urli and J. W. Corbett (IOP, Bristol, 1977), p. 465.
[20]M. G. Burt, J. Phys. C **13**, 1825 (1980).
[21]A. Nouailhat, F. Litty, S. Loualiche, P. Leyral, G. Guillot, J. Phys. **43**, 815 (1982).
[22]E. O. Kane, in *Semiconductors and Semimetals* (Academic, New York, 1966), Vol. 1, p. 75.
[23]S. Loualiche, Ph.D. thesis, University of Lyon, 1982.

[24]S. Loualiche, G. Guillot, A. Nouailhat, M. Gavand, A. Laugier, and J. Bourgoin, J. Appl. Phys. **53**, 8691 (1982).
[25]F. Bassani, in *Semiconductors and Semimetals,* Ref. 22, Vol. 1, p. 75.
[26]A. M. Stoneham, *Theory of Defects in Solids* (Clarendon, Oxford, 1975); J. C. Bourgoin and M. Lannoo, *Point Defects in Semiconductors II,* Vol. 35 of *Springer Series in Solid State Science,* edited by M. Cardona (Springer, New York, 1983).
[27]J. C. Slater, *Quantum Theory of Atomic Structure* (McGraw-Hill, New York, 1960), Vol. 1, p. 369.
[28]G. D. Watkins, Phys. Rev. Lett. **33**, 223 (1974).
[29]D. Pons and J. Bourgoin, Lund Conference, 1981 (unpublished).
[30]D. V. Lang, in *Proceedings of the International Conference on Radiation Effects in Semiconductors, Dubrovnik, 1976,* Ref. 19, p. 70.
[31]L. C. Kimerling and D. V. Lang, in *Proceedings of the International Conference on Lattice Defects in Semiconductors, Freiburg, Germany, 1974* (IOP, London, 1975), p. 589.
[32]D. V. Lang, L. C. Kimerling, and Y. S. Leung, J. Appl. Phys. **47**, 3587 (1976).
[33]D. Pons, A. Mircea, and J. Bourgoin, J. Appl. Phys. **51**, 4150 (1980).
[34]S. Loualiche, G. Guillot, and A. Nouailhat, Solid State Commun. **44**, 41 (1982).
[35]G. M. Martin and S. Makram-Ebeid, in Proceedings of the International Conference on Defects in Semiconductors, Amsterdam [Physica **116B**, 371 (1983)].
[36]D. Pons, in *Defects and Radiation Effects in Semiconductors,* edited by R. R. Hasiguti (IOP, London, 1981), p. 269.
[37]D. Pons, P. Mooney, and J. C. Bourgoin, J. Appl. Phys. **51**, 2038 (1980).
[38]D. Pons and J. Bourgoin, Phys. Rev. Lett. **47**, 1293 (1981).
[39]S. Loualiche, G. Guillot, A. Nouailhat, and J. Bourgoin, Phys. Rev. B **26**, 7090 (1982).
[40]J. L. Pinsard and A. Zylberstejn, in *GaAs and Related Compounds, 1980* (IOP, Bristol, 1981), p. 435.
[41]S. Loualiche, A. Nouailhat, and G. Guillot, Solid State Electron. **25**, 577 (1982).
[42]D. Pons (private communication).
[43]G. Bachelet, G. A. Baraff, and M. Schlüter, Phys. Rev. B **24**, 975 (1981), and references therein.
[44]M. Lannoo and G. Allan, Phys. Rev. B **25**, 4089 (1982).
[45]J. J. Markham, Rev. Mod. Phys. **31**, 956 (1959).
[46]M. H. L. Pryce, *Phonons in Perfect Lattices and in Lattices with Point Imperfections* (Oliver and Boyd, Edinburgh, 1966).
[47]M. Lannoo (unpublished).
[48]G. D. Watkins, in *Proceedings of the International Conference on Lattice Defects in Semiconductors, Freiburg, Germany, 1974,* Ref. 31, p. 1.
[49]J. van der rest and P. Pecheur, in Ref. 35, p. 121.
[50]G. A. Baraff, E. O. Kane, and M. Schlüter, Phys. Rev. Lett. **43**, 956 (1979); Phys. Rev. **21**, 3563 (1980); **21**, 5662 (1980).